Statistical Texture Image Classification Using Two-Dimensional Nonminimum-Phase Fourier Series Based Model

Chii-Horng Chen and Chong-Yung Chi *
Department of Electrical Engineering, National Tsing Hua University
Hsinchu, Taiwan, Republic of China
Tel: 886-3-5731156, Fax: 886-3-5715971, E-mail: cychi@ee.nthu.edu.tw

Abstract

Using the 2-D extension of Chi's real 1-D parametric nonminimum-phase Fourier series based model (FSBM) for or as an approximation to any arbitrary nonminimum-phase linear time-invariant (LTI) systems, we propose a system identification algorithm for 2-D nonminimum-phase linear shift-invariant (LSI) systems supported by some simulation results. The estimated 2-D FSBM parameters and second- and higher-order statistics obtained using the proposed algorithm constitute effective features for texture image classification supported by some experimental results.

1. Introduction

Chi [1,2] proposed a real 1-D parametric nonminimum-phase Fourier series based model (FSBM) for or as an approximation to any arbitrary nonminimum-phase linear time-invariant (LTI) systems. This model is applicable in a variety of statistical signal processing areas such as system identification, deconvolution and equalization, and spectral estimation. Recently, a real 2-D maximum phase - minimum phase (MX-MN) FSBM for linear shift-invariant (LSI) systems was proposed by Chi and Hsi [3] with application to 2-D texture image synthesis. This paper proposes a 2-D minimum phase - allpass (MP-AP) FSBM and then a 2-D system identification algorithm is proposed for the estimation of the FSBM parameters. The estimated FSBM parameters and the associated second- and higher-order statistics are then used for texture image classification.

*The research described in this paper was supported by the National Science Council under Grant NSC 88-2219-E-007-019.

2. 2-D MP-AP FSBM

The 2-D MP-AP nonminimum-phase FSBM for LSI systems is defined through the following frequency response:

$$\begin{aligned} H(\omega_1,\omega_2) &= H^*(-\omega_1,-\omega_2) \\ &= H_{\mathrm{MP}}(\omega_1,\omega_2)\cdot H_{\mathrm{AP}}(\omega_1,\omega_2) \end{aligned} \tag{1}$$

where $H_{\mathrm{MP}}(\omega_1,\omega_2)$ is a 2-D minimum-phase FSBM given by

$$\begin{aligned} &H_{\mathrm{MP}}(\omega_1,\omega_2) \\ &\quad = \exp\left\{ \sum\sum_{(i_1,i_2)\in\Omega(p_1,p_2)} \alpha_{i_1,i_2} e^{-j(i_1\omega_1+i_2\omega_2)} \right\} \end{aligned} \tag{2}$$

and $H_{\mathrm{AP}}(\omega_1,\omega_2)$ is a 2-D allpass FSBM given by

$$\begin{aligned} &H_{\mathrm{AP}}(\omega_1,\omega_2) \\ &\quad = \exp\left\{ j \sum\sum_{(i_1,i_2)\in\Omega(p_1,p_2)} \beta_{i_1,i_2} \sin(i_1\omega_1+i_2\omega_2) \right\} \end{aligned} \tag{3}$$

in which α_{i_1,i_2} and β_{i_1,i_2} are real-valued and $\Omega(p_1,p_2)$ is a truncated asymmetric half plane given by

$$\begin{aligned} \Omega(p_1,p_2) = \{&(i_1,i_2) : i_1 = 1\sim p_1, i_2 = -p_2 \sim p_2\} \\ &\cup \{(i_1,i_2) : i_1 = 0, i_2 = 1 \sim p_2\} \end{aligned} \tag{4}$$

It can be easily shown that the region of support of the minimum-phase system $h_{\mathrm{MP}}[m,n]$ is the right-half plane (i.e., $\Omega(\infty,\infty)$) and the leading coefficient $h_{\mathrm{MP}}[0,0] = 1$. The 2-D MP-AP nonminimum-phase FSBM $H(\omega_1,\omega_2)$ given by (1) shares the following characteristics of Chi's 1-D FSBM when used in statistical signal processing areas mentioned above:

(C1) System magnitude and phase responses of the FSBM $H(\omega_1,\omega_2)$ are characterized by α_{i_1,i_2}'s and $(\beta_{i_1,i_2} -$

α_{i_1,i_2})'s, respectively. When $\alpha_{i_1,i_2} = 0$, $h[m,n]$ is a 2-D allpass system; when $\beta_{i_1,i_2} = 0$, $h[m,n]$ is a 2-D minimum-phase system.

(C2) The FSBM $H(\omega_1, \omega_2)$, that can be causal or noncausal, is guaranteed (bounded-input bounded-output) stable since it is a continuous function of (ω_1, ω_2), so is the inverse system $1/H(\omega_1, \omega_2)$.

3. Identification of 2-D FSBM

Assume that we are given a set of non-Gaussian measurements $x[m,n]$ as follows:

$$x[m,n] = u[m,n] * h[m,n] \tag{5}$$

where $u[m,n]$ is a real, zero-mean, independent identically distributed (i.i.d.) non-Gaussian random field and $h[m,n]$ is a real 2-D system impulse response. Moreover, assume that the order parameters p_1 and p_2 are given in advance. The MP parameters α_{i_1,i_2} can be estimated using the following algorithm:

Algorithm 1. Estimation of $H_{\text{MP}}(\omega_1, \omega_2)$.

Let $v_{\text{MP}}[m,n]$ is a 2-D minimum-phase FSBM given by

$$V_{\text{MP}}(\omega_1, \omega_2) = \exp\left\{ \sum\sum_{(i_1,i_2)\in\Omega(p_1,p_2)} \widetilde{\alpha}_{i_1,i_2} e^{-j(i_1\omega_1 + i_2\omega_2)} \right\} \tag{6}$$

Then find the optimum $\widetilde{\alpha}_{i_1,i_2}$ by minimizing

$$J_{\text{MSE}} = E\{e^2[m,n]\} \tag{7}$$

where

$$e[m,n] = x[m,n] * v[m,n] \tag{8}$$

It can be shown that the optimum $\widehat{V}_{\text{MP}}(\omega_1, \omega_2)$ is an optimum linear prediction error (LPE) filter with

$$\widehat{V}_{\text{MP}}(\omega_1, \omega_2) = 1/H_{\text{MP}}(\omega_1, \omega_2) \tag{9}$$

i.e., $\widehat{\widetilde{\alpha}}_{i_1,i_2} = -\alpha_{i_1,i_2}$.

The AP parameters β_{i_1,i_2} can be estimated using the following algorithm:

Algorithm 2. Estimation of $H_{\text{AP}}(\omega_1, \omega_2)$.

(S1) Estimate α_{i_1,i_2} and obtain $e[m,n] \approx u[m,n] * h_{\text{AP}}[m,n]$ using Algorithm 1.

(S2) Process $e[m,n]$ using an allpass filter (a 2-D allpass FSBM)

$$V_{\text{AP}}(\omega_1, \omega_2) = \exp\left\{ j \sum\sum_{(i_1,i_2)\in\Omega(p_1,p_2)} \widetilde{\beta}_{i_1,i_2} \sin(i_1\omega_1 + i_2\omega_2) \right\} \tag{10}$$

such that the absolute Mth-order ($M \geq 3$) cumulant

$$J_{\text{CUM}} = |C_M\{y[m,n]\}| \tag{11}$$

of the allpass filter output signal

$$y[m,n] = e[m,n] * v_{\text{AP}}[m,n] \tag{12}$$

is maximum.

It can be shown [4] that the optimum

$$\widehat{V}_{\text{AP}}(\omega_1, \omega_2) = 1/H_{\text{AP}}(\omega_1, \omega_2) \tag{13}$$

i.e., $\widehat{\widetilde{\beta}}_{i_1,i_2} = -\beta_{i_1,i_2}$.

For finite data $x[m,n]$, the second-order and higher-order cumulants used in J_{MSE} (see (7)) and J_{CUM} (see (11)), respectively, must be replaced with the associated sample cumulants that are highly nonlinear functions of FSBM parameters. Therefore, gradient type optimization algorithms are needed for finding the minimum and maximum of J_{MSE} and J_{CUM}, respectively. Nevertheless, the proposed two algorithms also have a computationally efficient parallel structure as Chi's 1-D FSBM identification algorithms [1,2].

4. Simulation results

This section presents some simulation results for 2-D system identification using the proposed algorithms. Figure 1 shows some simulation results using Algorithm 2 with $p_1 = p_2 = 5$ and $M = 3$ for the case that $u[m,n]$ is a zero-mean, exponentially distributed i.i.d. random field, and $h[m,n]$ is a 2-D ARMA system taken from [5]. Figure 1(a) shows the true impulse response $h[m,n]$ and Figure 1(b) shows the average of ten independent estimates $\widehat{h}[m,n]$ for SNR = 20 dB (white Gaussian noise) . One can see that the result shown in Figure 1(b) is a good approximation to that shown in Figure 1(a). These simulation results support that the proposed Algorithms 1 and 2 are effective.

5. Texture image classification

As reported in [6], Gaussianity and linearity tests indicate that a texture image can be modeled as a 2-D LSI

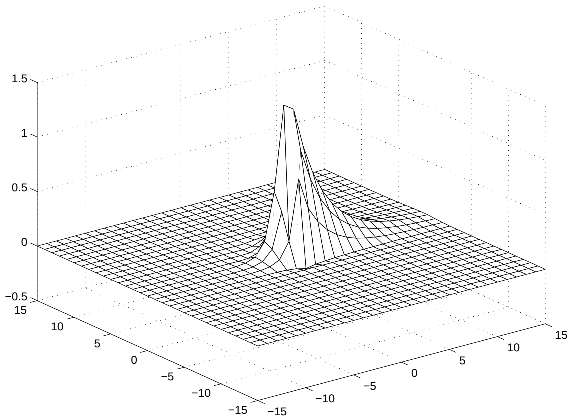

(a)

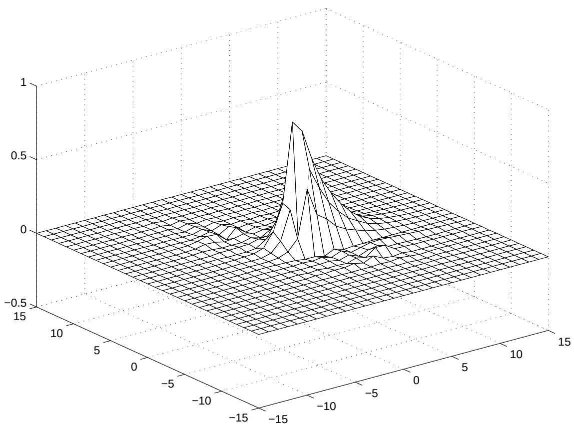

(b)

Figure 1. Simulation results using Algorithm 2. (a) The true impulse response $h[m,n]$ and (b) the average of ten independent impulse response estimates $\widehat{h}[m,n]$.

system (2-D texture image model) driven by an i.i.d. non-Gaussian random field. Accordingly, the proposed Algorithms 1 and 2 can be applied to obtain the following feature vectors for texture image classification:

$\boldsymbol{\theta}_1$: FSBM parameters α_{i_1,i_2} for all $(i_1,i_2) \in \Omega(p_1,p_2)$ obtained using Algorithm 1 and σ_e^2/σ_x^2, where σ_x^2 and σ_e^2 are the variances of $x[m,n]$ and $e[m,n]$, respectively.

$\boldsymbol{\theta}_2$: FSBM parameters α_{i_1,i_2} for all $(i_1,i_2) \in \Omega(p_1,p_2)$ and $\Lambda(y[m,n])$ obtained using Algorithm 2 where

$$\Lambda(y[m,n]) = \frac{E\{y^3[m,n]\}}{E\{y^2[m,n]\}^{3/2}} \qquad (14)$$

is the normalized third-order cumulant of $y[m,n]$.

Next, let us present some experimental results of texture image classification with features obtained using the proposed Algorithms 1 and 2. For a comparison, Kashyap and Chellappa's approximate maximum-likelihood (AML) algorithm [7] was also used to obtain the following feature vector for texture image classification:

$\boldsymbol{\theta}_3$: AR parameters a_{i_1,i_2} for all $(i_1,i_2) \in \bar{\Omega}(p_1,p_2)$ and ρ/σ_x^2 where

$$\bar{\Omega}(p_1,p_2) = \{(i_1,i_2) : |i_1| \le p_1, |i_2| \le p_2, \\ (i_1,i_2) \ne (0,0)\} \qquad (15)$$

and ρ is the residual power associated with a symmetric toroidal lattice SAR model.

The leave-one-out strategy and distance classifier [8] were used to perform classification using twelve different 512×512 texture images taken from the USC-SIPI Image Data Base. Each 512×512 texture image is segmented into sixteen 128×128 nonoverlapping subimages constituting a texture image class. Therefore, $192 = 16 \times 12$ subimages classifications were performed by the classifier. Tables 1, 2 and 3 show the classification results using the feature vectors $\boldsymbol{\theta}_1$ ($p_1 = p_2 = 3$), $\boldsymbol{\theta}_2$ ($p_1 = p_2 = 3, M = 3$), and $\boldsymbol{\theta}_3$ ($p_1 = p_2 = 2$), respectively. Each row of these tables includes numbers of classifications (over a 16-member subimage class) belonging to each of the 12 classes. From Tables 1, 2 and 3, one can see that the classifier using $\boldsymbol{\theta}_1$ (6 misclassifications) performs nearly as well as using $\boldsymbol{\theta}_2$ (4 misclassifications) and much better than using $\boldsymbol{\theta}_3$ (31 misclassifications). These results (as shown in Tables 1 and 2) justify that the FSBM parameters together with the associated second- and higher-order statistics are effective for texture image classification.

6. Conclusions

We have presented a 2-D system identification algorithm (Algorithm 2) using the 2-D FSBM given by (1) and its efficacy is supported by some simulation results. The FSBM parameters together with the associated statistics ($\boldsymbol{\theta}_1$ and $\boldsymbol{\theta}_2$) obtained by Algorithms 1 and 2 are effective features for texture image classification, as exhibited by the experimental results.

References

[1] C.-Y. Chi, "Fourier series based nonminimum phase model for second- and higher-order statistical signal processing," *Proc. 1997 IEEE Signal Processing Workshop on Higher-Order Statistics,* July 21-23, 1997, pp. 395-399.

[2] C.-Y. Chi, "Fourier series based nonminimum phase model for statistical signal processing," to appear in *IEEE Trans. Signal Processing.*

[3] C.-Y. Chi and C.-H. Hsi, “2-D blind deconvolution using Fourier series based model and higher-order statistics with application to texture synthesis,” *Proc. Ninth IEEE SP Workshop on SSAP,* Portland, Oregon, USA, Sept. 14-16, pp. 216-219.

[4] H.-M. Chien, H.-L. Yang and C.-Y. Chi, “Parametric cumulant based phase estimation of 1-D and 2-D nonminimum phase systems by allpass filtering,” *IEEE Trans. Signal Processing,* vol. 45, no. 7, pp. 1742-1762, July 1997.

[5] J. K. Tugnait, “Estimation of linear parametric models of nonGaussian discrete random fields with application to texture synthesis,” *IEEE Trans. Image Processing,* vol. 3, no. 2, pp. 109-127, March 1994.

[6] T.E. Hall and G.B. Giannakis, “Bispectral analysis and model validation of texture images,” *IEEE Trans. Image Processing,* vol. 4, pp. 996-1009, July 1995.

[7] R. L. Kashyap and R. Chellappa, “Estimation and choice of neighbors in spatial-interaction models of images,” *IEEE Trans. on Information Theory,* vol. 29, no. 1, pp. 58-72, Jan. 1983.

[8] R. L. Kashyap, R. Chellappa and A. Khotanzad, “Texture classification using features derived from random field models,” *Pattern Recognition Letters,* vol. 1, no. 1, pp. 43-50, 1982.

Table 1. Classification experiment using feature vector $\boldsymbol{\theta}_1$.

Texture size: 128×128, Misclassifications: 6 of 192												
Texture	1	2	3	4	5	6	7	8	9	10	11	12
1. grass	15	0	0	0	0	0	0	0	0	0	0	1
2. treebark	0	16	0	0	0	0	0	0	0	0	0	0
3. straw	1	0	13	0	0	1	0	0	0	0	0	1
4. herringbone	0	0	0	16	0	0	0	0	0	0	0	0
5. wool	0	0	0	0	16	0	0	0	0	0	0	0
6. leather	0	0	0	0	0	16	0	0	0	0	0	0
7. water	0	0	0	0	0	0	15	1	0	0	0	0
8. wood	0	0	0	0	0	0	0	16	0	0	0	0
9. raffia	0	0	0	0	0	0	0	0	16	0	0	0
10. brickwall	0	0	0	0	0	0	0	0	0	16	0	0
11. plastic	0	1	0	0	0	0	0	0	0	0	15	0
12. sand	0	0	0	0	0	0	0	0	0	0	0	16

Table 2. Classification experiment using feature vector $\boldsymbol{\theta}_2$

Texture size: 128×128, Misclassifications: 4 of 192												
Texture	1	2	3	4	5	6	7	8	9	10	11	12
1. grass	16	0	0	0	0	0	0	0	0	0	0	0
2. treebark	0	16	0	0	0	0	0	0	0	0	0	0
3. straw	1	0	14	0	0	1	0	0	0	0	0	0
4. herringbone	0	0	0	16	0	0	0	0	0	0	0	0
5. wool	0	0	0	0	16	0	0	0	0	0	0	0
6. leather	0	0	0	0	0	16	0	0	0	0	0	0
7. water	0	0	0	0	0	0	14	1	0	1	0	0
8. wood	0	0	0	0	0	0	0	16	0	0	0	0
9. raffia	0	0	0	0	0	0	0	0	16	0	0	0
10. brickwall	0	0	0	0	0	0	0	0	0	16	0	0
11. plastic	0	0	0	0	0	0	0	0	0	0	16	0
12. sand	0	0	0	0	0	0	0	0	0	0	0	16

Table 3. Classification experiment using feature vector $\boldsymbol{\theta}_3$

Texture size: 128×128, Misclassifications: 31 of 192												
Texture	1	2	3	4	5	6	7	8	9	10	11	12
1. grass	13	0	0	0	0	1	0	0	0	0	2	0
2. treebark	0	15	0	0	0	0	0	0	1	0	0	0
3. straw	2	0	12	0	0	1	0	0	0	0	0	1
4. herringbone	0	0	0	16	0	0	0	0	0	0	0	0
5. wool	0	0	0	4	12	0	0	0	0	0	0	0
6. leather	0	0	0	4	0	12	0	0	0	0	0	0
7. water	0	0	0	0	0	0	10	2	1	3	0	0
8. wood	0	0	0	0	0	0	0	16	0	0	0	0
9. raffia	0	0	0	0	0	0	0	0	16	0	0	0
10. brickwall	0	0	0	3	0	0	0	0	1	12	0	0
11. plastic	0	3	0	0	0	0	0	0	0	0	11	2
12. sand	0	0	0	0	0	0	0	0	0	0	0	16